



وزارة التعليم العالي والبحث
العلمي
جامعة المثنى
كلية العلوم
قسم الفيزياء

porous silicon fundamentals and applications

بحث مقدم الى قسم الفيزياء في كلية العلوم بجامعة المثنى كجزء
من متطلبات نيل شهادة البكالوريوس في قسم الفيزياء

اعداد الطالب

1- علي سمس عبيد

2- زينب ضامن سنيم

بإشراف

ا.م.د موفق فاضل جدوع

الاهداء

إلى صاحب السيرة العطرة، والفكر المستنير؛

فلقد كان له الفضل الأوّل في بلوغي التعليم العالي

(والدي الحبيب)، أطال الله في عُمره.

إلى من وضعتني على طريق الحياة، وجعلتني رابط الجأش،

وراعتني حتى صرت كبيراً

(أمي الغالية)، طيّب الله ثراها.

إلى إخوتي؛ من كان لهم بالغ الأثر في كثير من العقبات والصعاب.

إلى جميع أساتذتي الكرام؛ ممن لم يتوانوا في مد يد العون لي

أهدي إليكم بحثي في.....

الشكر والتقدير

بسم الله الرحمن الرحيم، والحمد لله رب العالمين الذي وفقنا وأعاننا على إنهاء هذا البحث والخروج به بهذه الصورة المتكاملة، فبالأمس القريب بدأنا مسيرتنا التعليمية ونحن تحسس الطريق برهبة وارتباك، فرأينا أن (قسم الفيزياء) هدفاً سامياً وغاية تستحق السير لأجلها،

وانطلاقاً من مبدأ أنه لا يشكر الله من لا يشكر الناس، فإننا توجه بالشكر الجزيل لجميع الاساتذة الذين رافقوني في مسيرتي لإنجاز هذا البحث وكانت لهم بصمات واضحة من خلال توجيهاتهم وانتقاداته البناءة والدعم الأكاديمي وبالأخص (ا.م.د. موفق فاضل جدوع)، كما نشكر عائلتنا التي صبرت وتحملت معنا ورفدتنا بالكثير من الدعم على جميع الأصعدة، ونشكر الأصدقاء والأحباب وكل من قدم الدعم المعنوي، والحمد لله رب العالمين.

Abstract

Porous silicon is a sponge-like structure of monocrystalline silicon which although accidentally discovered, soon became one of the most well-researched silicon structures. Its properties and applications Its unique properties have led to a variety of applications in the electronics industry. Since it is compatible with silicon microfabrication methods, porous silicon is ideal for use in sensors, solar cells, and high-power lasers. These materials also make for great materials for biomedical and electronic devices, enabling researchers to produce highly efficient electronic components. These advances in technology have made it a popular choice for sensors and electronics. have been the main subject of several books and more than a dozen review articles. porous silicon fabrication has though more than 20 different routes have been developed to synthesize this material. This Research briefly discusses the properties of porous silicon, describes its fabrication methods, and introduces its applications.

الخلاصة

السيليكون المسامي هو هيكل شبيه بالإسفنج من السيليكون أحادي البلورية والذي على الرغم من اكتشافه بالصدفة، سرعان ما أصبح أحد أكثر هياكل السيليكون بحثاً جيداً. خصائصه وتطبيقاته أدت خصائصه الفريدة إلى مجموعة متنوعة من التطبيقات في صناعة الإلكترونيات. نظراً لأنه متوافق مع طرق التصنيع الدقيق للسيليكون، فإن السيليكون المسامي مثالي للاستخدام في أجهزة الاستشعار، والخلايا الشمسية، والليزر عالي الطاقة. تُعد هذه المواد أيضاً مواد رائعة للأجهزة الطبية الحيوية والإلكترونية، مما يتيح للباحثين إنتاج مكونات إلكترونية عالية الكفاءة. جعلت هذه التطورات التكنولوجية منها خياراً شائعاً لأجهزة الاستشعار والإلكترونيات. كانت الموضوع الرئيسي للعديد من الكتب وأكثر من اثنتي عشرة مقالة مراجعة. لقد تم تطوير أكثر من 20 طريقاً مختلفاً لتركيبة هذه المادة في تصنيع السيليكون المسامي. يناقش هذا البحث بإيجاز خصائص السيليكون المسامي، ويصف طرق تصنيعه، ويقدم تطبيقاته

List of Figures

Figure 1-1 network of nanometer-sized silicon regions surrounded by void space...**10**

Figure 1-2 electrochemical anodization**10**

Figure 2-1 Electrochemical cell configurations used for the fabrication of PSi.....**14**

Figure 2-2 Divalent electrochemical dissolution of a silicon atom in HF solution....**16**

List of Tables

Table 2-1 properties of mesoporous silicon in comparison with of bulk silicon.....**18**

Table 2-2 PSi samples by FTIR measurements.....**19**

List of Contents

| | |
|---|----|
| Research Title..... | 1 |
| Dedication..... | 2 |
| Acknowledgement..... | 3 |
| Abstract..... | 4 |
| List of Figures..... | 5 |
| List of Tables..... | 6 |
| list of contents..... | 7 |
| List of Abbreviations..... | 8 |
| 1. Chapter 1: Introduction | |
| 1.1.Introduction..... | 9 |
| 1.2.History of Porous silicon..... | 11 |
| 2. Chapter 2: Fabrication and Properties | |
| 2.1.Fabrication of porous silicon..... | 12 |
| 2.1.1. Anodic etching..... | 13 |
| 2.1.2. Drying Techniques..... | 16 |
| 2.1.3. Oxidation Techniques..... | 17 |
| 2.2.Properties of porous silicon | 18 |
| 2.2.1. Structural Properties..... | 19 |
| 2.2.2. Chemical Properties..... | 19 |
| 3. Chapter 3: Applications | |
| 3.1.Applications..... | 20 |
| 3.1.1. optoelectronic applications..... | 20 |
| 3.1.2. Micro-optics..... | 21 |
| 3.1.3. Energy conversion..... | 21 |
| 3.1.4. Microelectronics..... | 21 |
| 3.1.5. Micromachining..... | 21 |
| 3.1.6. Biotechnology..... | 22 |
| References..... | 25 |

List of Abbreviations

| Abbreviations | definition |
|---------------|--|
| PSi | porous silicon |
| LEDs | light-emitting diodes |
| HF | hydrofluoric acid |
| SOI | silicon-on-insulator |
| DMF | dimethylformamide |
| EXAFS | extended X-ray absorption fine structure |
| XEOL | X-ray excitation of optical luminescence |
| BET | Brunauer–Emmett–Teller method |
| FTIR | Fourier transform infrared |
| SEM | scanning electron microscopy |
| SIMS | secondary ion mass spectrometry |
| PS-FP | Porous silicon Fabry-Pérot |
| PBG | Photonic bandgap |
| PEC | Photo-electrochemical cells |
| PCL | polycaprolactone |
| PPF | polypropylene fumarate |

Chapter 1: Introduction

1.1. Introduction

Silicon is at the heart of the microelectronics revolution. Its dominance over other semiconductors is intimately tied to its superior materials and processing properties and to the tremendous base of technology that has developed around it. Another semiconductor is not likely to displace silicon as the material of choice in electronic applications. Silicon, however, is an extremely inefficient light emitter, and for this reason has not enjoyed the same level of dominance in optical applications. The importance of developing a technology that would allow optical and electronic devices to be easily and inexpensively integrated on a silicon wafer has long been recognized. Such an advance would have a significant impact on display, communications, computer and a host of related technologies. In fact, a degree of optoelectronic integration on silicon wafers has been achieved. For example, high-quality optical detectors can be fabricated from silicon, and silicon charge-coupled device detector arrays are in common use. However, complete integration of optics and electronics requires putting light-emitting diodes (LEDs) and semiconductor lasers on the same wafer that contains detectors and electronic components. In today's technology, light-emitting semiconductor devices are fabricated almost exclusively from direct-bandgap compound semiconductors such as gallium arsenide and indium phosphide, which have much higher optical efficiency than silicon. Direct integration of compound semiconductor devices on a silicon wafer has proven to be very problematic. An alternative solution to this problem is to improve the efficiency of silicon itself, or to develop an optically efficient silicon-compatible material. Considerable research has been directed at this approach using techniques that range from the engineering of superlattices and quantum wells composed of silicon, germanium and carbon to the doping of silicon with optically efficient rare earth atoms such as erbium. (See reference 1 for discussions of many of these approaches.) Researchers have made progress with many of these techniques, but room-temperature efficiencies sufficiently high to challenge compound semiconductor materials have until recently appeared to be out of reach. In the fall of 1990, however, Leigh Canham of the UK's Defence Research Agency reported that one could obtain visible room-temperature photoluminescence from porous silicon layers formed on the surface of a silicon wafer.² The light-emitting properties that Canham reported for porous silicon were intriguing for several reasons. First, the emission energy was well above the bandgap of bulk silicon. Second, the energy (or color) could be tuned throughout the visible spectrum by changing the preparation conditions, an important consideration for display technologies that require red, green and blue devices. Finally, the quantum efficiency was comparable to that of direct-bandgap compound semiconductors. Canham's paper generated worldwide

speculation that a silicon-based optoelectronic technology was at hand, and it kicked off a flurry of research activity directed at porous silicon. Six years have passed since the initial report of room-temperature photoluminescence from porous silicon, and steady progress has been made in uncovering the fundamental properties of the mechanism of luminescence. Porous silicon's suitability for optoelectronic applications has also been an active area of research, and room temperature LEDs with efficiencies greater than 0.1%—as well as test structures that integrate LEDs with electronic devices—have been fabricated. In this article, we summarize the status of the field and discuss issues that remain to be resolved if porous silicon is to provide the missing link between electronic and optoelectronic integration.

Porous Silicon:

Described simply, porous silicon is a network of nanometer-sized silicon regions surrounded by void space (figure 1). A porous silicon film is typically prepared by electrochemical anodization of the surface of a silicon wafer. Figure (2) a is a schematic diagram of an electrochemical cell used to prepare porous silicon by anodic etching. Although interest in the light-emitting properties of porous silicon is a rather recent development, porous silicon itself was discovered in 1956 during a study of methods for electropolishing silicon. [1] The relationship between fabrication conditions and the structural and

electronic properties of porous silicon were examined extensively in subsequent work. The current density, hydrofluoric acid concentration, presence or absence of illumination during etching and, in particular, the doping type and resistivity of the silicon influence the morphology of the porous layer. For example, lightly doped p-type material tends to produce a spongelike pore morphology, whereas n-type material and heavily doped p-type silicon tend to give rise to dendritic or columnar features. Porosities (the fraction of void space) typically range from 50% to greater than 90%, with light emission generally occurring more efficiently for higher porosity.



Figure 1

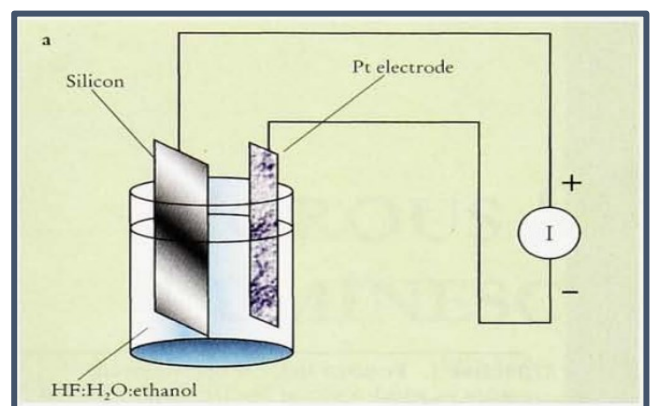


Figure 2

◆ Pore size distribution in porous silicon

The term porous silicon refers to very different types of materials which are obtained by electrochemical etching of silicon, and it is now well known that the characteristics of the so-formed materials are very dependent on the type and resistivity of the original silicon substrate and on the electrochemical parameters used during the anodization process. Therefore, the porosity value is a macroscopic parameter which does not give information about the microstructure of the layer. A much better knowledge of the porous structure is obtained if the pore sizes and their distribution in the material can be determined. However, this information is not so easy to obtain, and very different methods have to be used, depending on the size range involved. Up to now, there has been no comprehensive study of the pore size

distributions in porous silicon, because of the large number of parameters which influence this characteristic. However, some general trends can be derived which are presented here for the different types of starting silicon substrates, after a short description of the methods which have been used.

1. THE DETERMINATION OF PORE SIZES

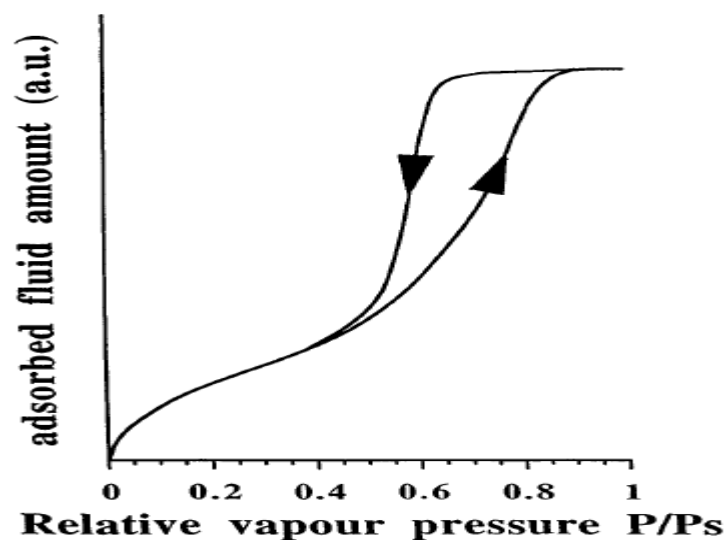
a) Macropores

Macropore distributions can be analysed by mercury porosimeter, but this method has not been used for porous silicon, possibly because it requires a relatively large porous volume. However, the pore dimensions are in a range which can be investigated by electron microscopy, and this is the only technique which has been used. Many papers report on pore observation by using both transmission (TEM) and scanning electron microscopy (SEM), and more recently high-resolution scanning microscopy. However, even though these techniques provide valuable information on the pore morphology, they only allow the determination of the average pore size range in the observed area, which is necessarily very localised.

b) Mesopores

Electron microscopy can still be used, but TEM or high-resolution SEM analysis are required. In this case, it is mainly the method based on the analysis of adsorption isotherms of gases at low temperature which has been used to give a more accurate determination of the pore size distribution. This method, which is widely used for the study of many porous media, was applied for the first time to porous silicon in 1983 . The adsorption isotherm of a gas by a porous solid presents a particular shape.

In the presence of mesopores, the physical adsorption of gases by a surface is increased relative to the nonporous surface by capillary condensation in pores, which starts at values of relative pressure where the smallest pores begin to be filled. FIGURE 1 shows a typical isotherm obtained on a porous silicon sample. The first part of the isotherm, up to a relative pressure of about 0.4, corresponds to the nitrogen adsorption on the porous surface; this regime allows the determination of the specific surface area of the sample by using the standard BET (Brumaire-Emmett-Teller) method . At higher relative pressures, the regime of sharp increase of the adsorbed volume corresponds to capillary condensation of the adsorbate in the pores. It is followed by a plateau which indicates the complete filling of all the pores with the liquid adsorbate. The volume of liquid corresponding to the amount of gas adsorbed at the plateau is the void volume in the sample and it allows the determination of the porosity. When the relative pressure decreases, evaporation of the condensed gas occurs, leading to the desorption branch which is shifted relative to the adsorption branch, so that the isotherm shows a hysteresis



loop. There are different methods to obtain the pore size distribution from the adsorption isotherms , either from the adsorption or desorption branch, and in the case of mesoporous silicon, it is the thermodynamical approach known as the BJH (Barrett-Joyner-Halenda) method which has been used

FIGURE 1 Schematic representation of the isotherm adsorption of nitrogen (at 77 K) obtained for a porous layer formed on a heavily doped p-type silicon substrate

The pore size has also been determined by X-ray experiments, by measuring the variations of the lattice parameter mismatch Aa/a during pentane adsorption and desorption as a function of the pressure. Large variations of Aa/a are observed at pressures where capillary condensation occurs inside the pores, with a hysteresis between increasing and decreasing pressures, just as for nitrogen adsorption experiments. Pore sizes have been determined from these experiments which agree well with the results of the BJH method. Other pore size determinations have been performed by small angle scattering of X-rays and nuclear magnetic resonance (NMR) spectroscopy, but it is always an average pore size which is obtained and not the size distribution. However, it has been reported that NMR surface studies using optically enhanced xenon as a surface probe may yield information about the pore size distribution. Very recently, thermophotometry has also been used. The method relies on the measurement of the shift of the transition temperature of a fluid confined in the pores, which is lowered when compared to the bulk fluid by an amount which is inversely proportional to the pore radius. By using differential scanning calorimetry (DSC) to study the liquid-solid phase transition of cyclohexane filling different porous silicon samples, the authors have determined pore sizes in very good agreement with the results obtained by adsorption isotherms

c) Micropores

The determination of pore size distribution in the range of micropores (radii below 1 nm) is very difficult. For a wholly microporous sample, the adsorption isotherm shows a different shape, with a rapid intake of nitrogen at very low relative pressures and no hysteresis upon gas desorption, and it is difficult to extract accurate pore size distribution from this type of isotherm [21]. In the presence of both micropores and mesopores, the problem is even more complicated as the addition of micropores results only in very small changes of the isotherm shape and in some modifications of the BET constants [21]. Electron microscopy also shows its limits: the pore dimensions are hardly resolved by high resolution SEM and, on the other hand, it becomes very difficult to avoid some degradation during sample preparation for TEM observation and only one paper reports on high resolution TEM observation of micropores. However, one study has shown that characterisation of microporous silicon could be achieved by using flow calorimetry. By measuring the heat of immersion of porous samples in alkanes and by comparing it with results obtained on silica lite, a microporous form of crystalline silicon dioxide, it was possible to determine that the pore size range of microporous silicon was that of 'super micropores', i.e. 1 - 2 nm width [22].

1.2. History of Porous silicon

Porous silicon was discovered in 1956 by Uhlir [2] while performing electropolishing experiments on silicon wafers using an electrolyte containing hydrofluoric acid (HF). He found that under the appropriate conditions of applied current and solution composition, the silicon did not dissolve uniformly but instead fine holes were produced, which propagated primarily in the $\langle 100 \rangle$ direction in the wafer. Therefore, porous silicon formation was obtained by electrochemical dissolution of silicon wafers in aqueous or ethanoic HF solutions .

In the 1970s and 1980s the interest on porous silicon increased because the high surface area of porous silicon was found to be useful as a model of the crystalline silicon surface in spectroscopic studies, as a precursor to generate thick oxide layers on silicon, and as a dielectric layer in capacitance -based chemical sensors [3] .

In the 1990s Leigh Canham published his results on red-luminescence from porous silicon, that was explained in terms of quantum confinement of carriers in nano-crystals of silicon which are present in the pore walls. Since that time, the interest of researchers and technologists to this material (and other porous semiconductors as well) is constantly growing and the number of publications dedicated to this class of materials increases every year. With the discovery of efficient visible light emission from porous silicon came an explosion of work focused on creating silicon-based optoelectronic switches, displays, and lasers. During the last twenty years, the optical properties of porous silicon have become a very intense area of research .

Chapter 2: Fabrication and Properties

2.1. Fabrication of porous silicon

Since 1956 that porous silicon was discovered, more than 20 methods have been developed to fabricate porous silicon structures. In this research, all manufacturing methods provided for porous silicon preparation will be mentioned, but we're going to go on to explain one way of manufacturing porous silicon

1. Anodization
2. Stain etching
3. Photoetching
4. Metal-assisted etching
5. Vapor etching
6. Reactive-ion etching
7. Spark erosion
8. Laser-induced plasma erosion
9. Oxidation of Rochow reaction byproduct
10. Ion implantation
11. Plasma hydrogenation
12. Laser ablation
13. High-density plasma deposition of silicon
14. Oblique-angle deposition
15. Unidirectional solidification of molten silicon
16. Porous silica reduction
17. Dealloying
18. Laser-induced silane decomposition
19. Electrodeposition
20. Mechanical synthesis
21. Annealing of ultrathin films of amorphous silicon
22. Using sacrificial template

2.1.1. Anodic etching

Before chemical mechanical polishing became dominant, electropolishing was used for planarization of silicon wafers. In electropolishing, a silicon wafer is placed in an electrochemical cell as the anode, a platinum electrode is utilized as the cathode, and hydrofluoric acid as the electrolyte. Passing electric current through the silicon wafer leads to dissolution of silicon atoms and removal of surface roughness if a critical current density (J_{PSL}) is exceeded. In 1956, something went wrong during an electropolishing process at Bell Labs, and the current in the cell reduced leaving a matt black, brown, or red layer on the surface of the wafer [4]. For more than a decade, it was believed that the matt dark layer formed on the silicon surface was a sub fluoride $(SiF_2)_x$ grown during the anodic dissolution. Later, it was proposed that the dark film was a dissolution/precipitation product resulted from a two-step disproportionation reaction. Finally, in 1969, it was discovered that the layer indeed has a porous structure formed by dissolution of silicon atoms in an electrochemical etching process [5].

Anodic etching, which is also called electrochemical etching, has been the most common method for the fabrication of porous silicon over the last 60 years. During these years, three electrochemical cell configurations have been utilized for the formation of porous silicon: lateral cell, single cell, and double cell. Lateral cell, which is the simplest electrochemical cell used for anodic etching of silicon, is shown in Figure 3(a). Silicon wafer about to be etched serves as the anode, platinum or any other conducting material resistant to hydrofluoric acid, like graphite, serves as the cathode electrode, and the cell body is made of acid-resistant polymers like PTFE. As the wafer is soaked in HF, any silicon surface that is exposed to the electrolyte is porosified as long as the current density remains below the critical value ($J < J_{PSL}$). The main advantages of the lateral cell are its simplicity and ability to anodize silicon-on-insulator (SOI) wafers. Its drawback is the nonuniformity in both porosity and thickness of the resulting layer. This inhomogeneity is due to a lateral potential drop across the wafer which leads to nonuniform current density and therefore nonuniform porosity and thickness [6].

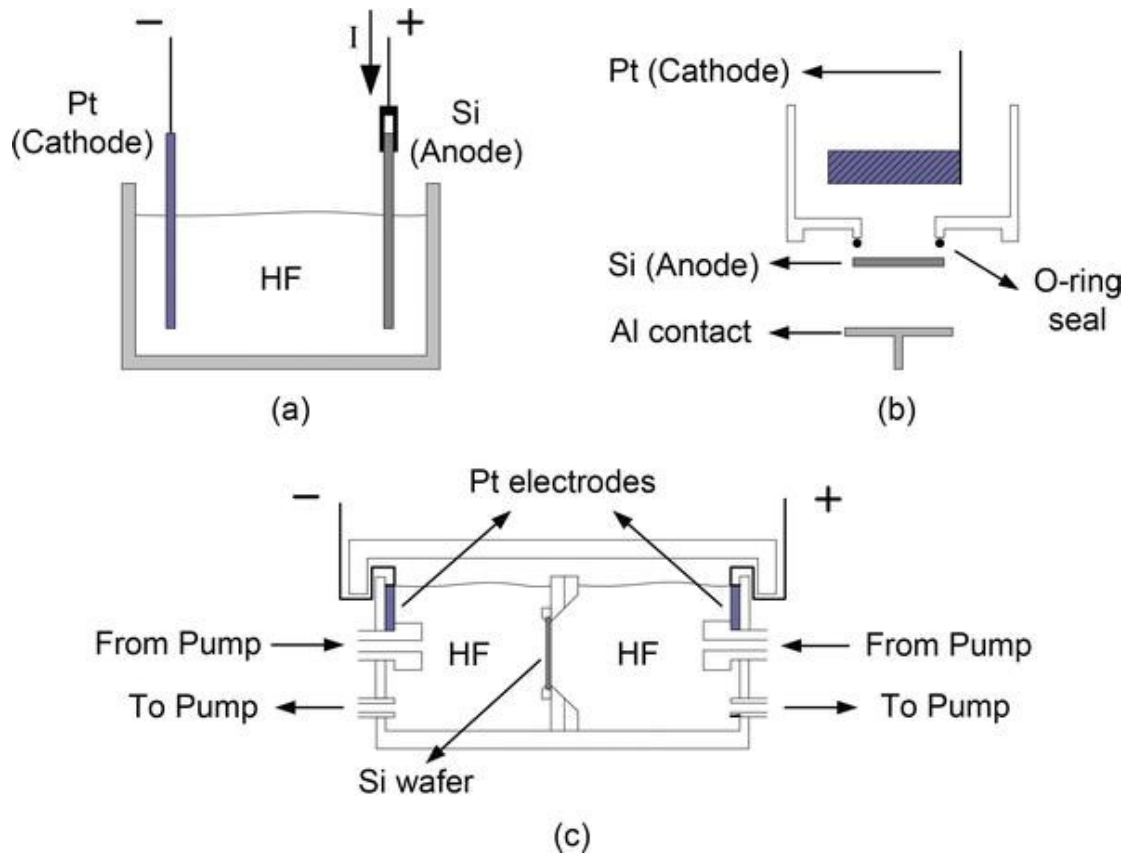


Figure 1.

Electrochemical cell configurations used for the fabrication of porous silicon: (a) lateral cell, (b) single cell, and (c) double cell.

The second configuration, single cell, shown in Figure 3(b), is the most common electrochemical cell used for the fabrication of silicon wafers. In order to provide uniform current density inside the silicon wafer, a back-side contact is used for the anode and the wafer is sealed so that only its front-side could be exposed to the electrolyte. Using this single cell configuration, acceptable porosity and thickness uniformity can be achieved for low resistivity silicon wafers. However, high resistivity wafers need high dose B or P ion implantation and subsequent annealing on their back-side to provide appropriate electrical contact to the external circuit. This implantation and subsequent annealing steps might be even followed by deposition of a thin layer of metal. Single cell configuration provides simultaneous control over porosity and thickness of the porous silicon film. Moreover, illumination which is necessary for n-type silicon wafers, can be easily performed in this cell. Using chemical pumps to circulate the electrolyte further improves the uniformity and minimizes the attachment of hydrogen bubbles to the silicon surface [7].

The last configuration, double cell, is designed to optimize the uniformity of porous silicon layer. It is composed of two half-cells separated by the silicon wafer about to be etched as illustrated in Figure 3(c). Large platinum electrodes which are immersed in both half-cells serve as anode and cathode. The electric current flows from one half-cell

to the other through the wafer. Hence, the front-side and back-side of the wafer act as local anode and local cathode. Chemical pumps are used to circulate the electrolyte between the half-cells to prevent any decrease in the local concentration of the electrolyte and remove the hydrogen bubbles. Here, electrolytic contact to the wafer reduces the nonuniformities associated with the back-side metal contact in the single cell approach. It also resolves the necessity of metallization in high resistivity wafers. By contrast, the equipment setup is complicated in comparison to the other electrochemical cells used for porosification [8]. In this configuration, if anodic etching under illumination is needed, the cell body should be made of transparent acid-resistant materials like PMMA.

The dissolution of silicon atoms by anodic etching can be controlled by either the current or the voltage of the electrochemical cell. Generally, constant current is preferred due to reproducibility and better controllability of porosity and thickness of the porous layer [9]. In the dissolution process, hydrogen gas is freed. The generated hydrogen bubbles are attached to the surface for some time preventing the electro-active species to reach the surface and interrupt the dissolution process. Addition of a surfactant like ethanol or methanol improves the penetration of the electrolyte into the pores and minimizes the hydrogen bubbles evolution [7]. Besides aqueous, ethanolic, or methanolic HF electrolytes, porous silicon can also be formed in the mixture of HF with metal oxides like manganese (IV) oxide MnO_2 , or certain organic compounds like acetonitrile CH_3CN and dimethylformamide (DMF).

Depending on the fact that electrochemical cell works either in electropolishing regime ($J > J_{\text{PSL}}$) or porosification ($J < J_{\text{PSL}}$), the charge transfer reactions that lead to the removal of the surface silicon atom, could be a tetravalent or divalent mechanism respectively. Figure 4 illustrates the divalent mechanism which leads to formation of porous silicon structures. In situ spectroscopy of silicon samples immersed in HF-based solutions has shown that the silicon surface is passivated by Si—H bonds [10]. As the Si—F bond (6 eV) is much stronger than the Si—H bond (3.5 eV), the possibility that the surface had been passivated by fluorine and then Si—F bonds were replaced by the Si—H ones, is ruled out. This led to the conclusion that if a surface silicon atom establishes a bond to a fluorine atom, it is immediately removed from the surface and the surface is passivated by hydrogen [11]. The dissolution of a surface atom begins when a hole traveling inside the silicon wafer reaches the interface of silicon and electrolyte (stage 1). At this point a bifluoride (HF_2^-) ion from the solution could attack Si—H bonds replacing one with a Si—F bond. Since the electronegativity of hydrogen is close to that of silicon, Si—H bonds are effectively unpolarized; therefore, they could not be influenced by bifluoride anions unless a hole was present. After the first Si—F bond

established, due to its polarizing effect, another bifluoride anion attacks the silicon atom releasing a hydrogen molecule as depicted in stage 3 of the figure. The polarization induced by the Si—F groups lowers the electron density of the silicon back-bonds and facilitates the dissolution of the loosely bounded silicon atom by HF. After the removal of a silicon atom, the remaining surface passivates with hydrides again (stage 5). The overall reaction in the divalent process can be summarized as Eq. (1):

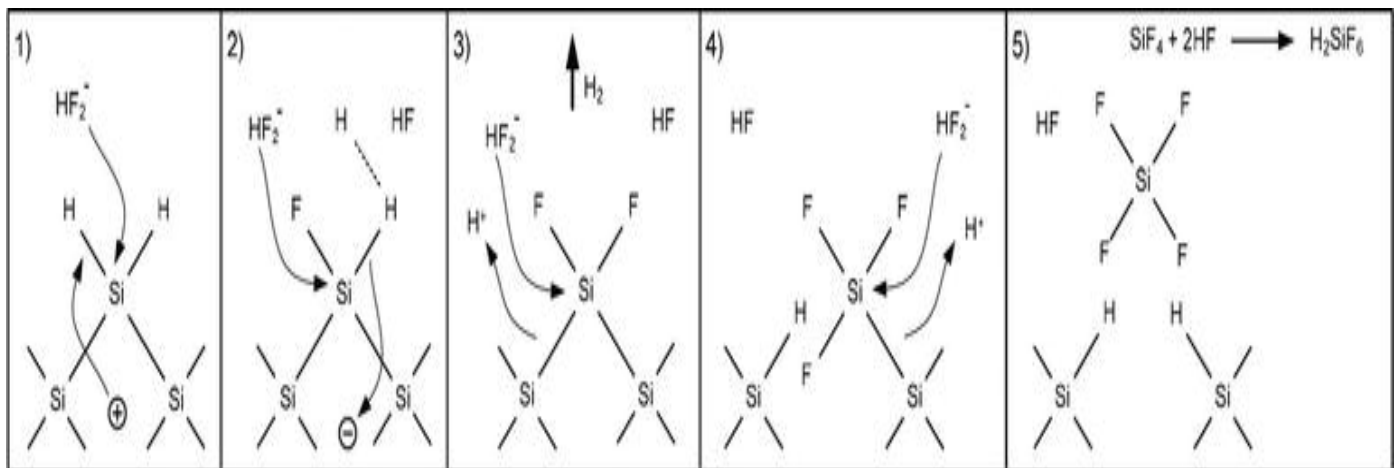
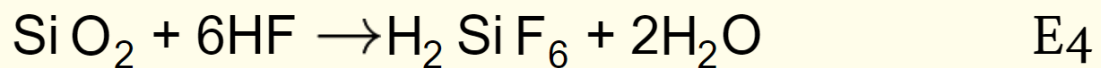


Figure 2. Divalent electrochemical dissolution of a silicon atom in hydrofluoric acid solution.

If the dissolved silicon atom was removed from a microscopically flat surface, its removal leaves a microroughness. This small topographical alteration changes the distribution of the electric field which increases the probability of presence of the holes. Hence, the etch rate at microroughness becomes greater than the surrounding flat areas. Accordingly, surface roughness increases and eventually a porous structure is formed.

Anodic etching is the most common method for the fabrication of chip-based n-type and p-type porous silicon. All classes of porosity can be realized by anodic etching with proper control over the porosity and thickness. Although there has been success in integration of anodically etched porous silicon structures with electronic circuitry, this fabrication method is not compatible with standard ULSI technology [12].

2.1.2. Drying Techniques

Due to large capillary stress, drying of samples is a critical step and can result in extended cracking if special procedures are not followed. Methods to reduce or eliminate the capillary stress include pentane drying, supercritical drying, freeze drying, and slow evaporation rates. Pentane drying is the easiest to implement. Pentane has a very low surface tension, and shows no chemical interaction with PSi (unlike ethanol).

Using pentane as drying liquid enables to strongly reduce the capillary tension, but since water and pentane are nonmiscible liquids, ethanol or methanol have to be used as intermediate liquids. Using this drying technique, P*Si* layers with porosity values up to 90% and thickness up to 5 mm exhibit no cracking pattern after drying. Supercritical drying requires a specific apparatus but is more effective in preventing cracking of the film so that P*Si* layers of porosity values up to 95% were demonstrated.

2.1.3. Oxidation Techniques

As soon as P*Si* samples are dried, hydrogen surface passivation is gradually replaced by native oxide.

This chemical change affects most P*Si* properties, for example, photoluminescence and electrical conductivity. Since the characteristics of the native oxide strongly depend on many factors such as the storage conditions, evolution of sample properties is often poorly characterizable. To stabilize P*Si* properties, oxidation is often used. Oxidation implies the formation of a layer containing the original Si atoms. Therefore, it also reduces the nanocrystallite size, with remarkable impact on photoluminescence emission energy (blue-shift). The employment of controlled oxidation procedures is therefore a valuable post-anodization option toward a better control of P*Si* properties and stabilization.

Tested oxidation procedures on P*Si* include anodic oxidation, chemical oxidation, thermal oxidation, plasma-assisted oxidation, and irradiation-enhanced oxidation. Anodic oxidation is an electrochemical process, in which oxide layers are formed with current injection. As such, the technique is structurally selective: more conductive paths get more oxidized. This selectivity is particularly interesting for lightemitting diode (LED) applications, where more conductive paths are usually associated to large injection channels, which are poorly luminescent, and their oxidation results in enhanced electroluminescence quantum efficiency. Another application of controlled oxidation – mostly thermal – is the fabrication of small, blue-luminescent P*Si* nanocrystallites.

2.2. Properties of porous silicon

Porous silicon structures, like other porous materials, are classified by their dominant pore dimensions. Structures with pore dimensions below 2 nm and above 50 nm are called microporous and microporous silicon, respectively; those lie between are called mesoporous silicon. Due to the extremely rich details with respect to the range of variations in pore size, shape, orientation, branching, interconnection, and distribution, morphology is the least quantifiable aspect of this material

Various morphologies and different pore dimensions give porous silicon extremely diverse structural, mechanical, optical, electrical, thermal, emissive, physiochemical, and biochemical properties. Table 1 compares the properties of mesoporous silicon with those of bulk silicon. As the structure and surface chemistry of porous silicon can be precisely controlled during properly chosen fabrication process and appropriate post-fabrication treatment, the material's properties can be tuned according to the desired application. Tuning of porous silicon properties can be performed by manipulating its structural parameters, altering its surface chemistry, or impregnating other materials [12].

| | Property | Bulk silicon | Mesoporous silicon |
|------------|----------------------------|--------------------------------------|---|
| Structural | Porosity | — | 20–95% |
| | Density | 2.33 g/cm ³ | 0.12–1.9 g/cm ³ |
| | Pore size (diameter) | — | 2–50 nm |
| | Surface area | — | 100–800 m ² /g |
| | Lattice structure | Diamond | Diamond |
| Mechanical | Young's modulus | 160 GPa | 1–100 GPa |
| | Hardness | 11.5 GPa | 0.2–10 GPa (layer) 0.05–1 GPa (composite) |
| | Yield strength | 7 GPa | — |
| | Fracture toughness | 0.6 MPam ^{1/2} | — |
| Optical | Bandgap | 1.1 eV | 1.1–3.2 eV |
| | Infrared refractive index | 3.5 | 1.1–3.0 |
| | Color | Gray | All colors (layer) Brown-yellow (particle) |
| | Reflectivity (500–1000 nm) | 10–35% | 0.1–10% |
| Electrical | Resistivity | 10 ² –10 ³ Ωcm | 10 ³ –10 ¹² Ωcm |
| | Free electron mobility | 1350 cm ² /Vs | 0.1–30 cm ² /Vs |
| | Hole mobility | 480 cm ² /Vs | 2–6 cm ² /Vs |
| | Dielectric constant | 11.5 | 2–8 |
| Thermal | Conductivity | 150 W/mK | 0.03–20 W/mK |
| | Melting point | 1414°C | 800–1414°C |
| | Specific heat | 0.7 J/gK | — |
| | Diffusivity | 0.8 cm ² /s | — |
| Emissive | PL wavelength | 1000–1200 nm | 400–1300 nm |
| | PL efficiency | 10–6 | 0.01–0.23 (films) |
| | | | 0.01–0.6 (suspensions) |

| | | | |
|----------------|--------------------------|-------------|-----------------------|
| | EL efficiency | 10–8 | 0.01–0.1 |
| Physiochemical | Isoelectric point | pH 1.6–2.5 | pH 1.6–7.7 |
| | Zeta potential (pH 7) | –(45–70) mV | – |
| | Surface wettability | 5–96° | <0.5–167° |
| Biochemical | Medical biodegradability | – | Months (implants) |
| | | | Days (microparticles) |
| | | | Hours (nanoparticles) |

Table 1. Tunable properties of mesoporous silicon in comparison with those of bulk silicon [12].

2.2.1 Structural Properties

Structural properties of P*Si* have been investigated by electron microscopy, scanning probe microscopy, X-ray scattering techniques, X-ray absorption techniques, and Raman spectroscopy. In particular, X-ray absorption spectroscopy can be performed not only by extended X-ray absorption fine structure (EXAFS) analysis, but also by X-ray excitation of optical luminescence (XEOL), a convenient tool for luminescent samples, in which absorption is probed via the measurement of the corresponding optical emission. A general feature resulting from the comparison of these techniques is that highly luminescent P*Si* is a composition of extensively connected Si crystals of nanometric dimensions (typically, 1–5 nm in radius). Sizes smaller than Si Bohr radius (~4.9 nm), imply significant quantum confinement effects. Raman measurements are also often used to demonstrate crystallinity in P*Si* skeleton and infer information on the size of Si nanocrystals.

Accurate determination of pore size distribution in mesoporous Si is usually given by the analysis of adsorption isotherms of gases at low temperature (Brunauer–Emmett–Teller, or BET, method). The physical adsorption by a porous surface is increased relative to a nonporous one because of capillary condensation in pores. This increase in adsorption starts when the gas pressure is high enough to fill the smallest pores.

Since the discovery of intense visible photoluminescence (PL) given by anodised porous Si, an extremely large amount of analytical work has been carried out on the material world-wide. This has been driven to a substantial extent by the potential for the fabrication of light-emitting optoelectronic devices, although there is also a deep fundamental interest in the mechanism of light emission. Many of the factors which have influenced this progress are considered in this book. The present data review focuses on the underlying structure of the porous material and considers the way in which this critically determines the luminescence behaviour.

2.2.1.1 ANALYTICAL TECHNIQUES

The structural characteristics of porous Si have been studied by a range of techniques. Direct imaging of the material can be carried out by scanning electron microscopy (SEM), although the resolution achievable (down to <2 nm) and the available contrast make it difficult to visualise the smallest structures. The latter are generally imaged by transmission electron microscopy (TEM), which permits studies with resolution down to atomic dimensions. However, samples for assessment must be thinned to electron

transparency and it is vital that the technique employed (usually ion milling or direct cleavage) introduces as little atomic-scale damage and disorder as possible. Indeed, rapid transfer of freshly-prepared samples to the vacuum of the microscope is essential to limit or even prevent unwanted surface oxidation. Of course, once a specimen is loaded into an electron microscope, additional investigations of elemental composition and electronic properties based on X-ray microanalysis, electron energy loss spectroscopy and cathodoluminescence spectroscopy and imaging are also possible. X-ray analytical methods have also been employed to provide much important structural information on porous Si [H]. Although the basic structure of porous Si is too small-scale to be imaged by X-ray topography, diffraction measurements permit the assessment of material crystallinity and lattice spacing. Furthermore, small angle scattering measurements allow the determination of nanostructure dimensions and alignments, the surface area per unit volume and the sharpness of the Si interface with internal voids [H]. Two methods based on X-ray absorption have been applied to porous Si analyses. In one case, the selective excitation of characteristic X-ray emission (monitored by photoelectron yield) with impressed X-ray absorption fine structure (XAFS) can give information on the bandgap and local atomic order of the material. In the other case, X-ray photoelectron spectroscopy is used to assess the chemical state of the probed atoms. A number of scanning probe microscopy techniques have been used in the study of porous Si. Atomic force microscopy (AFM) gives a direct surface image but with restricted lateral resolution and scanning tunnelling microscopy (STM) provides imaging information related to the surface electronic structure. Both types of image may be distorted due to the relatively large dimensions of the scanning tip. Lastly, it is important to note that electron spin resonance (ESR) and nuclear magnetic resonance (NMR) have supplied information on odd electron centres, pore geometry, etc

2.2.1.2 POROUS SILICON FROM SINGLE CRYSTAL MATERIAL

After the anodization of single crystal Si, early X-ray diffractometry work on p⁺ and p['] material has showed that the porosities lattice is dilated with respect to the substrate and that the expansion increases with increasing porosity. TEM studies have demonstrated that pore microstructure depends upon crystalline Si resistivity: p⁺ (001) Si yields a mesoporous structure with pores in a range around 10 nm elongated along [001] and presenting a characteristic branching 'fir-tree-like' morphology, while p["] (001) Si yields finer, less regular pores with a 'coral-like' microporous microstructure on a scale of 2 nm. For comparison, anodization of n⁺ Si yields mesoporous material similar to that for p⁺ Si, although n["] Si anodised in the dark or with appropriate illumination of the backside of the wafer gives pores of up to 100 nm or greater dimensions (macropores). The latter often have crystallographic ally aligned edges and the pores themselves are found to follow <001>-type directions, even when these are inclined to the wafer surface normal as for (110) Si. Macropores are of potential importance for VLSI trench formation since pore positions can be lithographically predetermined allowing regular

arrays to be produced. When the porosity of the material is increased to very high values (approximately 70% or greater) very strong, efficient PL emission is observed [21]. Although it was originally proposed that this phenomenon is due to recombination of excited carriers quantum-confined in the remaining crystalline skeleton, evidence for this was only indirect and further detailed structure studies have been required. The first definitive study of luminescent material employed TEM of specimens rapidly transferred to the microscope after production by direct cleavage from as anodised Si. This demonstrated that the porous matrix is composed of undulating, interconnected columns of crystalline Si with diameters down to below 3 nm. The crystallinity of the material was

confirmed by electron diffraction patterns, which gave evidence for some distortion and nanoscale fragmentation of the structure. The latter is likely to be promoted by liquid surface

tension forces during drying after anodization and can be eliminated by supercritical drying under pressure in CO₂, When this is carried out, Si with porosities up to greater than 95% can be produced with little damage due to drying, with diameters in the 3 - 5 nm range. The single crystal diffraction pattern, but there is no evidence for the presence of misoriented crystallites. Following the original observations, many TEM studies have confirmed the presence of interconnected nanocrystalline structural units in luminescent porous Si, usually in columnar arrays although occasionally in platelet form. Furthermore, some experimental results indicate that a proportion of an amorphous phase can be distributed within the nanocrystalline matrix and, for example, amorphous sheaths have been seen on the crystalline skeleton. However, in view of the earlier results and when account is taken of potential structural damage caused by e.g. ion milling (for thin TEM specimen preparation) and oxidation in the air after preparation, it is evident that as anodised luminescent porous Si generally contains only restricted amounts of any amorphous phase. Although thin porous Si films

formed by the alternative fabrication method of 'stain etching' do contain amorphous material. nanocrystals still remain and can account for PL emission observed [23]

◆ Elastic properties of porous silicon

There have been very few investigations of the elastic properties of porous silicon (PS), which are, however, expected to differ drastically from those of bulk silicon. Moreover, the use of PS for some applications is limited by the mechanical instability of this fragile material (upon drying for instance).

Young's moduli of different PS samples were measured by means of four different techniques: they appear to be drastically dependent on the porosity and on the doping level (p or p⁺-type).

For instance, highly porous silicon layers exhibit very low values of Young's modulus. The analysis of the data relating to the elastic properties of PS is reported in this paper, including a short discussion about the specific problem of the elastic properties of porous materials

A. X-RAY DIFFRACTION STUDY

The first investigation of the elastic properties of PS was performed by Birla et al on p+- type PS material by using X-ray diffraction. This paper was the first to show that PS material behaves as a nearly perfect single crystal. Indeed, they showed that when using a high-resolution X-ray diffraction experiment, the rocking curve is composed of two well defined Bragg peaks, related to the silicon substrate and to the PS layer. Therefore, they concluded that porosity affects the PS lattice by producing a slight expansion. The angular distance between the two peaks is directly related to the lattice mismatch parameter $\Delta a/a$. The latter induces a curvature R_c of the whole silicon wafer, which is given by:

$$R_c = \frac{1}{6} \frac{E}{E_p} \frac{1 + \nu_p}{1 - \nu} \frac{a}{\Delta a} \frac{t_s^2}{t_p}$$

where E and E_p are the Young's moduli, and ν and ν_p the Poisson ratios, respectively, for bulk and porous silicon, while t_s and t_p are the thicknesses of the silicon wafer and the PS layer. The measurement of the wafer curvature and lattice parameters (either strained or relaxed) for different (hkl) reflections allowed information about the Young's modulus and Poisson ratio of PS layers to be determined. It was then clearly shown for the first time that PS material is less

stiffer than bulk silicon (i.e. with lower Young's modulus values). Moreover, this study also gave a Poisson ratio value for a 54% porosity p+-type PS sample: $\nu_p \gg 0.09$ which is much smaller than that of bulk silicon: $\nu \ll 0.26$ (to this author's knowledge this is the only estimate reported on PS material). [24]

◆ Thermal conductivity of porous silicon

Thermal conductivity is one of the most important physical parameters of any material. While the electronic and optical properties of porous silicon have been investigated by a large number of authors, the thermal properties have received much less interest. Nevertheless, as soon as porous silicon is to be applied in a device, thermal management must be considered. Due to its porous structure, the material shows a low thermal conduction; in its nanoporous form it can be even considered to be a good thermal insulator. Concerning luminescence, especially electroluminescence within LEDs, this can cause a severe problem. Since the quantum efficiency of porous silicon LEDs is still rather low, a lot of heat is generated which has to flow through the porous layer. On the

other hand, for microsystems and sensor applications, the low thermal conductivity can be used to form a thermally isolating layer on silicon. In this way, thermally isolated structures for thermal sensors can be placed on a hard material instead of the thin membranes normally used for this purpose. These sensors should be more robust than the membrane types.

A. ELECTRICALLY INDUCED THERMAL WAVE DATA

Measurements of thermal properties have only recently been published. The numerical values scatter strongly, which is expected due to the different morphologies of the material.

The first reported values have been measured by the IFT in Munich. The method used is the analysis of thermal waves in the sample. The waves are generated by a thin film heater on top of the porous layer. Another resistor on the back of the wafer is used for measuring the amplitude and phase of the waves after they have travelled through the whole sample. From these data the thermal conductivity is calculated. The results have to be discussed with respect to the morphology of the different samples. [25]

2.2.2 Chemical Properties

Surface chemical composition of PSi is best probed with Fourier transform infrared (FTIR) spectroscopy. FTIR signal in PSi is larger and easier to measure than in bulk Si due to much larger specific area. Chemical bonds and their IR resonance positions detected in PSi are shown in Table 2. In fresh, as-prepared samples, oxygen is normally absent, the dominant bonds being Si-H_x groups (x= 1, 2, or 3). Aging is observed as a slow replacement of H by O bonds in PSi. Also, luminescence fatigue is explained by photochemical reactions occurring on the surface of the Si nanocrystal [14].

Table 2 Wave number positions and attributions of the absorption peaks observed in several PSi samples by Fourier transform infrared absorption FTIR measurements

| Peak position (cm ⁻¹) | Attribution | Peak position (cm ⁻¹) | Attribution |
|-----------------------------------|-------------------------------------|-----------------------------------|---------------------------------------|
| 3610 | OH stretch (SiOH) | 1463 | CH ₃ asymmetric deformed |
| 3452 | OH stretch (H ₂ O) | 1230 | SiCH ₃ bending |
| 2958 | CH stretch (CH ₃) | 1056–1160 | SiO stretching in O–SiO and C–SiO |
| 2927 | CH stretch (CH ₂) | | |
| 2856 | CH stretch (CH) | 979 | SiH bending in Si ₂ –H–SiH |
| 2248 | SiH stretch (O ₃ –SiH) | 948 | SiH bending in Si ₂ –H–SiH |
| 2197 | SiH stretch (SiO ₂ –SiH) | 906 | SiH ₂ scissor |
| 2136 | SiH stretch (Si ₂ O–SiH) | 856 | SiH ₂ wagging |
| 2116 | SiH stretch (Si ₂ H–SiH) | 827 | SiO bending in O–Si–O |
| 2087 | SiH stretch (Si ₃ –SiH) | 661 | SiH wagging |
| 1720 | CO | 624 | SiH bending in (Si ₃ SiH) |

The internal surface of porous silicon (PS) layers varies from about 200 to 600 m²/cm³ depending on the dopant level of the substrate from which they are formed. Such an inner surface contains a high density of sites for original impurities such as hydrogen and fluorine coming from the electrolyte used for the anodic dissolution. After the formation, the layers are generally kept in ambient air for a few hours and even a few days. During this period, natural oxidation occurs and also contamination by chemical species from the atmosphere.

The optical and electrical properties depend on these impurities. The luminescence properties for example depend on the presence of hydrogen which passivates the silicon dangling bonds, and also on the presence of oxides which change the crystallite size and introduce surface states which may be non-radiative (Si dangling bonds) or radiative recombination centers. Moreover, luminescence in the blue spectral range appears from aged PS which has been attributed to the presence of oxide. PS is also known to be sensitive to moisture. The conductivity for example is increased by the presence of acetone vapors or ammonia, so sensors can be realised. It is hence indispensable to know the chemical composition of PS layers when studying their physical properties. In this Data Review we discuss the main results concerning the chemical composition of freshly etched ('fresh') PS, together with the experimental techniques used. We focus on material that has only been exposed to ambient air for minutes to hours prior to analysis.

2.2.2.1 ORIGINAL IMPURITIES

A. Hydrogen

By an in-situ potential-modulated Fourier transform IR (FTIR) experiment, Venkateshwara Rao Et Al have shown the presence of SiH_x (x = 1, 2, 3) groups on the inner surface of PS layers during the electrochemical dissolution process. After formation, once the layers are dried, the majority of these SiH_x groups remain at the surface for weeks and even for months. The presence of such groups has been shown by many authors using IR absorption and nuclear magnetic resonance, for example, shows the transmission FTIR spectrum for a self-supported p⁺-type PS sample in the SiH stretch frequency region: the lines at 2090 cm⁻¹, 2102 - 2117 cm⁻¹ and 2140 cm⁻¹ correspond to the stretch modes of SiH, SiH₂ and SiH₃ hydride species respectively. The full width at half maximum (FWHM) of the different lines is broadened compared to the one corresponding to a supported porous layer which is probably due to the visible distortion of the PS layer when it is separated from its substrate. which corresponds to a supported p⁺ layer. In order to avoid absorption by the substrate, the thickness of the porous layer was the highest possible (~300 μm), but in this case the most intense SiH lines saturate so that the porous layer was annealed at 450°C for 1 hr. One can still observe the presence of SiH and SiH₂ stretching modes with FWHM of about 2 cm

Chapter 3: Applications

3.1. Applications

Due to its high chemical reactivity and rapid oxidation, porous silicon was being utilized for device isolation. By the end of the 1980s, porous silicon had also been used for other purposes like the realization of SOI substrates and the formation of a buffer layer in epitaxial growth of compound semiconductors on silicon substrates. However, it was only after the discovery of strong photoluminescence in porous silicon that the material attracted broad attention. Since then porous silicon has been used for the fabrication of gas sensors, humidity sensors, biosensors, light emitting structures, optical waveguides, distributed Bragg reflectors, Fabry-Pérot resonators, photonic crystals, flat panel displays, optical and acoustic filters, ultrasound generators, and many other devices. Even though optoelectronics has remained the main research area of porous silicon, recently, the material has found application in other areas like medicine, diagnostics, cosmetics, consumer care, and nutrition. In contrast to the conventional chip-based applications, these new areas rely on porous silicon powders and independent structures. In this section, we briefly discuss the application domains of porous silicon and the reader is encouraged to refer to the literature dedicated to porous silicon applications (for example, see [13]).

3.1.1. optoelectronic applications

A. LEDs.

the first publication on the formation of the electroluminescent devices based on porous silicon was made by Richter et al. and later by Koyama and Koshida .

Those were Au/PS/c-Si Schottky diodes with rather low quantum efficiency $10^{-5} \pm 10^{-4} \%$. Since then, continuous efforts of these and many other research groups have resulted in continuous improvement of the efficiency and reliability of PS-based LEDs.

Soon after the first attempts to build conventional Schottky type diodes. introduced LEDs with porous p-n contact. They have yielded increase of the efficiency up to $10^{-2} \%$. have optimized this concept of LED structure and built the device with external quantum efficiency as high as 0.2% at working voltage of 2 V and continuous operation of up to 100 h in vacuum. The first samples of LEDs with porous p-n junctions lacked stability while working in the open environment. Linnros and Lalic have shown that the environmental stability of LEDs is much improved if the pulsed mode of operation for Au/(p⁺-n) PS/n⁺Si/Al is used. Onset time of establishing EL was about 9 ms and decay time of about 25 ± 30 ms, presumably due to the high impedance of the diode. Details of pulsed operation of PS-based LEDs were studied by Wang et al. Delay of

electroluminescence signal from pulse-polarized diode was studied and ascribed to trapping of injected carriers in thin oxide layer at the Au/PS Schottky contact. Lazarouk et al. reported the formation of very stable Al/PS LEDs using CVD deposition of silicon onto sapphire substrates, formation of porous silicon layer, and aluminum contacting pattern (using a deposition of Al film and its local anodic oxidation). While reverse-biased, the diodes emit white light, presumably due to the excitation of surface plasmons in oxide (Al₂O₃ or SiO₂) near the edges of Al metallization stripes where the maximum local electric field is concentrated. Tsybeskov et al. have performed a partial oxidation of PS material to stabilise the electroluminescence yield from poly-Si/p+-PS/p-PS/Si diode structure. The device has shown tunable EL yield in visible, high quantum efficiency (0.1%) at a working voltage of 2V. Although essential progress has been achieved in the fabrication of LEDs based on porous silicon, further work is necessary towards increasing their stability, quantum efficiency and speed.

B. Waveguides

Since the first report on the use of porous silicon as an optical waveguide medium in the 90s, significant development has been made towards the understanding and applicability of such material. Different groups have studied the fabrication of porous silicon waveguides and their basic properties (modes, losses).

The infiltration of liquids in the pores resulting in an induced phase shift and/or variation in the guided light intensity allows the use of porous silicon waveguide as sensors. For example, the introduction of solvents (acetone, methanol, and propan-2-ol) into the pores is shown to dramatically reduce the loss of the waveguides in a reversible manner. Waveguides based on porous silicon multilayers allow the micromachining of photonic integrated circuits as it can be used to confine, manipulate, and guide the photons. Waveguides based on multilayers have attracted a great interest because their guiding mechanism is completely different to the conventional waveguides based on total internal reflection but these waveguides made of porous silicon have not been widely reported. [15]

C. field emitters

A fabrication technology for porous silicon (PS) field emitters for display applications is described. Silicon blunt emitters prepared on p-type silicon wafers of 30 Ω cm resistivity were covered with a thin layer of porous silicon using an electrochemical anodization in ethanoic hydrofluoric solution. A PS layer with similar characteristics was also prepared on flat silicon surfaces. The PS layer morphology was investigated by scanning electron microscopy (SEM). The composition of the PS layers after the stabilization treatments was analyzed by secondary ion mass spectrometry (SIMS). Similar values of the vacuum field emission current were obtained for both cases of PS

on silicon blunt tips and on flat surfaces. The oxidized porous silicon layers did not show vacuum field emission properties at all. Good field emission results were obtained on samples that were immediately processed to prevent the PS oxidation or on samples with a stabilized porous surface. [16]

3.1.2. Micro-optics

A. Fabry-Pérot (PS-FP) filters

Porous silicon Fabry-Pérot (PS-FP) filters operating in the long wavelength infrared (LWIR) range are demonstrated and studied. Porous silicon (PS) offers many advantages for such filters, including improved optical and mechanical properties compared to other LWIR filter materials, and the ability to modulate porosity to form multilayer structures that are compatible with conventional semiconductor technologies [17].

B. Photonic bandgap (PBG) structures

Photonic bandgap (PBG) structures have remarkable optical properties that can be exploited for biosensing applications. We describe the fabrication of 1-D PBG biosensors using porous silicon. The optical properties of porous silicon PBGs are sensitive to small changes of refractive index in the porous layers, which makes them a good sensing platform capable of detecting binding of the target molecules to the bioreceptors. The material nanostructure and device configuration that lead to optimum performance of the devices are investigated in detail by modeling the optical response. It is shown that porous silicon based PBG sensors are useful for detecting biological matter, from small molecules to larger proteins [18].

3.1.3. Energy conversion

A. Photo-electrochemical cells

Wireless photovoltaic (PEC) devices promise easy device manufacturing as well as reduced waste. It fabricates a free-standing ion exchange material-embedded photovoltaic cell structure with micron-sized pores, to overcome 1) pH gradient formation due to long-distance ion transport, 2) product junction, and 3) parasitic light absorption by applying a modular catalyst. [19].

3.1.4. Microelectronics

- A. **Micro-capacitor** High specific surface area
- B. **Insulator layer** High resistance
- C. **Low-k material** Electrical properties

3.1.5. Micromachining

A. Thick sacrificial layer

Surface micromachining is an established micro technology. The process is only limited by sacrificial layer thickness and sometimes a disturbing surface topology. This paper describes an innovative surface micromachining technology. Standard surface micromachining allows layer thickness of a few micrometer. Using porous silicon as sacrificial layer, it is possible to create any layer thickness up to 100 micrometers . Thick porous silicon sacrificial layers are used to combine the advantages of standard surface micromachining with the advantages of bulk micromachining. The problems resulting from surface topology are eliminated by using ion implanted masks. Based on different porous silicon formation mechanism for n- and p-type silicon, it is possible to use n-implanted layers as masking material during the anodization of p-type silicon, resulting in a planar surface. For this masking technology, no additional masking layers are required. For free standing membrane generation it is possible to deposit e.g. a PECVD-layer on top of the porous silicon layer. If required, e.g. to protect free standing structures during following process steps from mechanical failures, it is possible to remove sacrificial layers with diluted alkaline solution in a final process step after dicing. A complete process flow has been developed for thick porous silicon layers up to 100 micrometers . The use of this sacrificial layer technology for thermally isolate gas sensor membrane fabrication and the detailed process parameters will be presented.

3.1.6. Biotechnology

A. Tissue bonding

Recently it was demonstrated that Si particles can be used in tissue engineering and orthopedics for the recovery of connective tissue elements. In particular, it was shown that porous Si promotes osteoblast growth by affecting the phase of bone mineralization. Usually, porous Si is used in a composite material, in combination with some biocompatible polymer. Polylactide, polydimethylsiloxane, polyethylene, or polycaprolactone can be used as such polymers. The combination of porous Si with biocompatible polymers has a number of advantages in comparison with the use of the components separately. It was shown that combination of porous Si with polycaprolactone (PCL) strengthens the material. In addition, Si/PCL composites are easily permeable to water, which contributes to natural biodegradation of Si. It was demonstrated that the rate of Si destruction is linearly dependent on its percentage in the composite and on the size of the composite. The composites consisting of porous Si and polypropylene fumarate (PPF) are being actively developed in the Ferrari laboratory. Researchers believe that the use of such material will allow patients to walk a few days after the administration of the composite. In this case porous Si fulfills a double function, i.e., carries the growth factors contributing to bone growth and incorporates itself into the bone tissue, ensuring its quick recovery.

B. biosensors

The modified Si particles can be used as biosensors for detecting proteins, antigens, or nucleic acid molecules. Since porous Si has a large surface area, it is possible to modify the particles by a large number of sensor molecules. An example of application of porous Si for detecting the MS2 viruses is given in. The possibility to detect the MS2 viruses in a solution using porous Si particles modified by rabbit anti- MS2 antibodies was shown. To this end, the viral particles stained by Alexa532 fluorescent dye were used. It was demonstrated that porous Si bound with anti- MS2 antibodies absorbs viruses considerably more effectively than then on modified Si particles. To determine the sensitivity of porous Si bound with antibodies to MS2, various concentrations of the virus were studied (from 1×10^6 to 2×10^6 PFU/mL). The dependence of fluorescence intensity of particles as a function of the virus concentration was found. In addition, silicon particles can be used for searching certain drug molecules (drug screening) and for diagnosing various diseases [20].

References

1. Reuben T. Collins, Philippe M. Fauchet, and Michael A. Tischler. Porous Silicon: From Luminescence to LEDs. *Phys. Today* 50(1), 24 (1997);
2. A. Uhlir, [Bell System Technology Journal](#), 35, p.333 (1956).
3. Anderson, R. C., Muller, R. S., & Tobias, C. W. (1989). Investigation of porous silicon for vapor sensing (No. UCRL-21267). Lawrence Livermore National Lab. (LLNL), Livermore, CA (United States); Berkeley Sensor and Actuator Center, CA (USA).
4. Uhlir Jr, A. (1956). [Electrolytic shaping of germanium and silicon](#). *Bell System Technical Journal*, 35(2), 333-347.
5. Zhang XG. [Morphology and formation mechanisms of porous silicon](#). *Journal of the Electrochemical Society*. 2004;151(1):C69-C80.
6. Halimaoui A. [Porous silicon formation by anodisation](#). In: Canham L, editor. *Properties of Porous Silicon*. UK: INSPEC; 1997. pp. 12-22
7. Fauchet PM et al. [Light-emitting porous silicon: Materials science, properties, and device applications](#). *IEEE Journal of Selected Topics in Quantum Electronics*. 1995;1(4):1126-1139.
8. Jung KH, Shih S, Kwong DL. [Development in luminescent porous Si](#). *Journal of the Electrochemical Society*. 1993;140(10):3046-3064. DOI: 10.1149/1.2220955
9. Korotcenkov G, Cho BK. [Silicon porosification: State of the art](#). *Critical Reviews in Solid State and Materials Sciences*. 2010;35(3):153-260. DOI: 10.1080/10408436.2010.495446
10. Niwano M, Miura T, Kimura Y, Tajima R, Miyamoto N. [Real-time, in situ infrared study of etching of Si \(100\) and \(111\) surfaces in dilute hydrofluoric acid solution](#). *Journal of Applied Physics*. 1996;79(7):3708-3713. DOI: 10.1063/1.361203
11. Lehmann V. [Electrochemistry of Silicon: Instrumentation, Science, Materials and Applications](#). Germany: Wiley-VCH; 2002
12. Canham L. Tunable properties of porous silicon. In: Canham L, editor. [Handbook of Porous Silicon](#). Switzerland: Springer; 2014. pp. 201-206
13. Canham L, editor. [Handbook of Porous Silicon](#). Switzerland: Springer; 2014. pp. 731-1008
14. G. Bassani, [Encyclopedia Dictionary of Condensed Matter Physics](#), Published by London, United Kingdom: Academic Press Inc.(London) Ltd, 2005
15. Xifré Pérez, Elisabet, 2007-06-22, DESIGN, FABRICATION AND CHARACTERIZATION OF POROUS SILICON MULTILAYER OPTICAL DEVICES, <https://www.tesisenred.net/handle/10803/8458?show=full>
16. E. Boswell, T. Y. Seong, and P. R. Wilshaw, 07 July 1994, Studies of porous silicon field emitters, <https://booksc.org/book/33085927/ab0986>
17. Yaman Afandi. Gia Parish. Adrian Keating, 1 December 2021, Micromachined porous silicon Fabry-Pérot long wavelength infrared filters, <https://www.sciencedirect.com/science/article/abs/pii/S0924424721005665#>
18. Huimin Ouyang, Philippe M. Fauchet, 10 November 2005, Biosensing using porous silicon photonic bandgap structures, <https://www.spiedigitallibrary.org/conference-proceedings-of-spie/6005/600508/Biosensing-using-porous-silicon-photonic-bandgap-structures/10.1117/12.629961.full?SSO=1>
19. Wouter J. C. Vijselaar, Paula Perez-Rodriguez, 27 March 2019, A Stand-Alone Si-Based Porous Photoelectrochemical Cell, <https://onlinelibrary.wiley.com/doi/full/10.1002/aenm.201803548>
20. de la Mora, M. B. , Ocampo, M., Doti, R., Lugo, J. E. , & Faubert, J. (2013). Porous Silicon Biosensors. In (Ed.), *State of the Art in Biosensors - General Aspects*. IntechOpen. <https://www.intechopen.com/chapters/40653>
21. Porous silicon / noble metal nanocomposites/for catalytic applications/Sergej Polisski/ A thesis submitted for the degree of Doctor of Philosophy /University of Bath/Department of Physics/September 2010
22. HERINO, R. Pore size distribution in porous silicon. Short Run Press Ltd.: London, 1997.

23. CULLIS, A. G. Structure and crystallinity of porous silicon. *Properties of Porous Silicon*, 1997, 18.
24. BELLET, D. Elastic properties of porous silicon. *Properties of Porous Silicon*, INSPEC, London, 1997, 127-131.
25. DROST, A., et al. Thermal conductivity of porous silicon. *Sensors and Materials*, 1995, 7: 111-111.